

Direct identification of continuous-time linear switched state-space models ^{*}

Manas Mejari ^{*} Dario Piga ^{*}

^{*} *IDSIA Dalle Molle Institute for Artificial Intelligence, USI-SUPSI,
Via la Santa 1, CH-6962 Lugano-Viganello, Switzerland. (e-mail:
{manas.mejari, dario.piga}@supsi.ch).*

Abstract: This paper presents an algorithm for direct *continuous-time* (CT) identification of *linear switched state-space* (LSS) models. The key idea for direct CT identification is based on an integral architecture consisting of an LSS model followed by an integral block. This architecture is used to approximate the continuous-time state map of a switched system. A properly constructed objective criterion is proposed based on the integral architecture in order to estimate the unknown parameters and signals of the LSS model. A coordinate descent algorithm is employed to optimize this objective, which alternates between computing the unknown model matrices, switching sequence and estimating the state variables. The effectiveness of the proposed algorithm is shown via a simulation case study.

Keywords: Continuous-time system estimation, Hybrid and switched systems modeling.

1. INTRODUCTION

1.1 Linear switched systems

Switched linear models belong to a class of hybrid systems, which consists of multiple linear subsystems and a switching signal dictating the *active* linear subsystem at each time instance. Such model class is widely used to describe the behavior of dynamical systems subject to abrupt changes, exhibiting both continuous and discrete dynamics. These changes can occur, for instance, due to sensor/actuator failures, external disturbances or a change in the operating point of a non-linear system.

Over the past few decades, switched linear models have found several applications in a variety of fields including, mobile communication (Abdollahi and Khorasani, 2011), signal processing (Doucet et al., 2001), computer vision and bio-tracking (Oh et al., 2008), energy disaggregation (Mejari et al., 2018), modeling human motion dynamics (Pavlovic et al., 2000), among many others.

1.2 On direct continuous-time identification

Concerning the identification of linear switched systems, majority of the approaches proposed in the literature have been developed for the identification of *discrete-time* (DT) models. Among these, we mention optimization based algorithms (Bako, 2011; Ohlsson and Ljung, 2013), recursive clustering-based approaches (Breschi et al., 2016; Mejari et al., 2020a), mixed-integer programming algorithms (Mejari et al., 2020b), Bayesian inference (Piga et al., 2020), algebraic-geometric approach (Vidal, 2008), which identify DT switched linear models in *input-output* (IO) form. Although IO models are able to describe the behavior of

the underlying system, often it is desirable to estimate state-space representations, as they are more convenient for stability analysis and controller synthesis of multi-input multi-output plants. To this end, realization theory and subspace based algorithms have been developed for DT switched linear state-space models, see (Bako et al., 2009; Petreczky et al., 2013; Verdult and Verhaegen, 2004).

In comparison with the large number of contributions dedicated to the estimation of DT switched models, very few works have addressed direct *continuous-time* (CT) identification of switched models. However, as discussed in (Garnier, 2015; Garnier and Wang, 2008; Piga, 2018) for *linear time-invariant* (LTI) models, direct identification of CT model from sampled data offers multiple advantages over the discrete-time case. Most of the physical systems are naturally modelled in continuous-time, and thus, the estimated parameters of CT models usually have a physical interpretation. Direct CT identification methods can also deal with non-uniformly sampled data, while discrete-time models implicitly rely on a fixed sampling time. Moreover, CT identification methods are generally more robust to numerical issues that may arise when using discrete-time methods in the case of high-frequency sampled data.

Motivated by these advantages, our goal in this paper is to develop an algorithm for direct CT identification for switched linear models. The core idea is based on the concept of *integral architecture*, recently introduced by the authors in Mavkov et al. (2020); Mejari et al. (2022) for identification of CT non-linear and LPV systems. In this work, we extend that methodology for *linear switched state-space* (LSS) model class.

1.3 Paper contributions and related works

We consider the problem of direct CT identification of LSS models which involves: estimating the matrices of

^{*} This work has been submitted to IFAC World Congress'23 for possible publication.

each LTI submodel, computing a discrete mode sequence which indicates the active submodel at a given time, and estimating the continuous state-sequence, from a given sampled IO data. The proposed solution is based on an integral architecture consisting of LSS model followed by an integral block, which is used to approximate the continuous state dynamics of an LSS system. A block coordinate descent algorithm is employed to optimize a properly constructed dual-objective criterion, which alternates between computing the unknown matrices, discrete mode sequence and estimating the states.

To the best of our knowledge, direct CT identification of switched linear models has been addressed very recently only in (Goudjil et al., 2020; Kersting and Buss, 2019; Du et al., 2021). These approaches, however, rely on strong assumptions imposed on the system’s signals. In particular, the CT identification method proposed in Goudjil et al. (2020) requires that the input signal exciting the system is sinusoidal. Then, by exploiting the linearity of subsystems, outputs of individual subsystems are estimated using a DT switched IO method. In the next stage, CT identification approaches developed for LTI models are employed to estimate model parameters based on estimated subsystem outputs. In Kersting and Buss (2019), parameter identifiers and concurrent learning is proposed based on the assumptions that discrete mode sequence as well as continuous states are measured. Integral concurrent learning is proposed in Du et al. (2021) relaxing the assumption of known switching sequence. However, the continuous state is assumed to be measured. To position our work w.r.t. these contributions, we do not impose any of the aforementioned assumptions required in (Goudjil et al., 2020; Kersting and Buss, 2019; Du et al., 2021), which are quite restrictive in practice. In particular, in our contribution the input signals used to excite the system are not restricted to sinusoidal inputs. On the contrary, any class of input signals which excite all modes of the system can be used. Furthermore, neither the discrete mode sequence nor the continuous state are assumed to be known. The proposed algorithm estimates both these signals along with the model matrices through a block coordinate-descent approach tailored to the considered identification problem.

The paper is organized as follows. The identification problem for LSS models is formalized in Section 2. The description of the integral architecture and details of proposed proposed identification algorithm are provided in Section 3. A simulation example is reported in Section 4.

2. PROBLEM FORMULATION

We consider a data-generating system \mathcal{S} governed by the following CT linear switched state-space representation:

$$\dot{\mathbf{x}}(t) = A_{\mathbf{s}(t)}\mathbf{x}(t) + B_{\mathbf{s}(t)}\mathbf{u}(t), \quad (1a)$$

$$\mathbf{x}(0) = \mathbf{x}_0, \quad (1b)$$

$$\mathbf{y}^o(t) = C_{\mathbf{s}(t)}\mathbf{x}(t) + D_{\mathbf{s}(t)}\mathbf{u}(t), \quad (1c)$$

where $\mathbf{x}(t) \in \mathbb{R}^{n_x}$ and $\dot{\mathbf{x}}(t) \in \mathbb{R}^{n_x}$ are the state vector and its time derivative, respectively; $\mathbf{x}_0 \in \mathbb{R}^{n_x}$ is the initial condition; $\mathbf{u}(t) \in \mathbb{R}^{n_u}$ is the system input; $\mathbf{s}(t) \in \{1, \dots, K\}$ is the switching signal and $\mathbf{y}^o(t) \in \mathbb{R}^{n_y}$ is the (noise-free) system output at time $t \in \mathbb{R}$. Note that,

the system is assumed to have K operating *modes*, each corresponds to an LTI state-space system with real-valued matrices $\{A_i, B_i, C_i, D_i\}_{i=1}^K$ of appropriate dimensions.

A training dataset \mathcal{D} of length N is gathered from the linear switched system \mathcal{S} defined in (1) at time instants $\{t_0 = 0, t_1, \dots, t_{N-1}\}$. The dataset consists of input and *noisy* output samples: $\mathcal{D} = \{\mathbf{u}(t_k), \mathbf{y}(t_k)\}_{k=0}^{N-1}$ with sampling time Δt . The measured output is corrupted by a zero-mean white Gaussian noise $\eta \sim \mathcal{N}(0, \sigma_\eta^2 I)$, *i.e.*, $\mathbf{y}(t_k) = \mathbf{y}^o(t_k) + \eta(t_k)$.

Problem 1. Given a training dataset \mathcal{D} , our goal is to identify a continuous-time linear switched state-space (LSS) model, such that the model output matches closely with the measured system output $\mathbf{y}(t)$.

The following assumptions are imposed on the system and signals in (1):

1. input signal $\mathbf{u}(t)$ can be reconstructed (or reasonably approximated) for all time instants $t \in [0, t_{N-1}] \subset \mathbb{R}$ from the measured samples $\{\mathbf{u}(t_k)\}_{k=0}^{N-1}$.
2. time evolution of the switching signal $\mathbf{s}(t)$ is stochastic, but it’s value does not change during the sampling interval Δt .
3. all K operating modes are distinguishable and sufficiently excited.

In the paper, we consider a constant sampling time Δt only to ease the notation. Nevertheless, the approach is valid also for varying sampling times.

In the next paragraph, we introduce an *integral architecture* for the identification of continuous-time LSS model.

3. CONTINUOUS-TIME IDENTIFICATION OF LSS MODELS

3.1 Integral architecture

In order to describe the continuous-time state dynamics in (1a), we define an LSS block $\mathcal{M}_x(\hat{\mathbf{x}}, \mathbf{u}, \hat{\mathbf{s}})$, which is fed by the system input $\mathbf{u}(t)$, (estimated) switching signal $\hat{\mathbf{s}}(t)$ and (estimated) state $\hat{\mathbf{x}}(t)$ at time t , and returns the estimated state time-derivative $\hat{\dot{\mathbf{x}}}(t)$, *i.e.*,

$$\mathcal{M}_x(\hat{\mathbf{x}}, \mathbf{u}, \hat{\mathbf{s}}) : \hat{\dot{\mathbf{x}}}(t) = \hat{A}_{\hat{\mathbf{s}}(t)}\hat{\mathbf{x}}(t) + \hat{B}_{\hat{\mathbf{s}}(t)}\mathbf{u}(t), \quad (2)$$

where $\hat{A}_i \in \mathbb{R}^{n_x \times n_x}$ and $\hat{B}_i \in \mathbb{R}^{n_x \times n_u}$ (for $i = 1, \dots, K$) are the model matrices to be identified. Similarly, the output equation in (1c) is represented by another block $\mathcal{M}_y(\hat{\mathbf{x}}, \mathbf{u}, \hat{\mathbf{s}})$, which is fed by the estimated state $\hat{\mathbf{x}}(t)$, input $\mathbf{u}(t)$ and estimated switching signal $\hat{\mathbf{s}}(t)$ and it returns the model output $\hat{\mathbf{y}}(t)$ at time t , *i.e.*,

$$\mathcal{M}_y(\hat{\mathbf{x}}, \mathbf{u}, \hat{\mathbf{s}}) : \hat{\mathbf{y}}(t) = \hat{C}_{\hat{\mathbf{s}}(t)}\hat{\mathbf{x}}(t) + \hat{D}_{\hat{\mathbf{s}}(t)}\mathbf{u}(t), \quad (3)$$

where the matrices $\hat{C}_i \in \mathbb{R}^{n_y \times n_x}$ and $\hat{D}_i \in \mathbb{R}^{n_y \times n_u}$ (for $i = 1, \dots, K$) have to be estimated from data.

For brevity, we introduce the following notation: $\Theta_x = \{\hat{A}_i, \hat{B}_i\}_{i=1}^K$, $\Theta_y = \{\hat{C}_i, \hat{D}_i\}_{i=1}^K$ and the mode sequence $\mathbf{S} = (\hat{\mathbf{s}}(0), \dots, \hat{\mathbf{s}}(t_{N-1}))$

The resulting continuous-time LSS model is then given by:

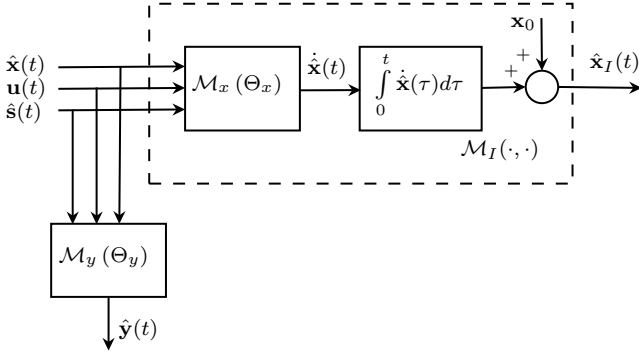


Fig. 1. Integral architecture for continuous-time LSS model identification.

$$\dot{\hat{\mathbf{x}}}(t) = \mathcal{M}_x(\hat{\mathbf{x}}(t), \mathbf{u}(t), \hat{\mathbf{s}}(t); \Theta_x(\hat{\mathbf{s}}(t))), \quad (4a)$$

$$\hat{\mathbf{x}}(0) = \hat{\mathbf{x}}_0, \quad (4b)$$

$$\hat{\mathbf{y}}(t) = \mathcal{M}_y(\hat{\mathbf{x}}(t), \mathbf{u}(t), \hat{\mathbf{s}}(t); \Theta_y(\hat{\mathbf{s}}(t))), \quad (4c)$$

where $\Theta_x(\hat{\mathbf{s}}(t))$ and $\Theta_y(\hat{\mathbf{s}}(t))$ denote the matrices $(\hat{A}_{\hat{\mathbf{s}}(t)}, \hat{B}_{\hat{\mathbf{s}}(t)})$ and $(\hat{C}_{\hat{\mathbf{s}}(t)}, \hat{D}_{\hat{\mathbf{s}}(t)})$ respectively, corresponding to the *active mode* $\hat{\mathbf{s}}(t)$ at time t . Note that, for the i -th active mode, *i.e.*, $\hat{\mathbf{s}}(t) = i$ at time t , the maps $\mathcal{M}_x(\cdot)$ and $\mathcal{M}_y(\cdot)$ are *linear functions* of the model matrices (A_i, B_i) and (C_i, D_i) respectively.

In this paper, we adopt a method originally introduced in Mavrov et al. (2020), which exploits the *integral form* of the Cauchy problem (4a)-(4b), by defining an *integral block* \mathcal{M}_I as:

$$\hat{\mathbf{x}}_I(t) = \mathcal{M}_I(\hat{\mathbf{x}}(t), \mathbf{u}(t), \hat{\mathbf{s}}(t); \Theta_x(\hat{\mathbf{s}}(t))) \quad (5)$$

with

$$\begin{aligned} \mathcal{M}_I(\hat{\mathbf{x}}(t), \mathbf{u}(t), \hat{\mathbf{s}}(t); \Theta_x(\hat{\mathbf{s}}(t))) \\ = \hat{\mathbf{x}}(0) + \int_0^t \mathcal{M}_x(\hat{\mathbf{x}}(\tau), \mathbf{u}(\tau), \hat{\mathbf{s}}(\tau); \Theta_x(\hat{\mathbf{s}}(\tau))) d\tau. \end{aligned}$$

The block diagram in Fig. 1 is a representation of (5), along with the output equation (4c) producing $\hat{\mathbf{y}}(t)$. Given the mode sequence \mathbf{S} , if the state $\hat{\mathbf{x}}(t)$ feeding the LSS model block $\mathcal{M}_I(\cdot)$ is actually generated by the model given in (4), then the state $\hat{\mathbf{x}}_I(t)$ exactly matches $\hat{\mathbf{x}}(t)$, *i.e.*,

$$\hat{\mathbf{x}}(t) = \hat{\mathbf{x}}_I(t) \quad \forall t \in [t_0, t_{N-1}]. \quad (6)$$

3.2 Fitting criterion

In the proposed scheme, the LSS model matrices Θ_x, Θ_y , the mode sequence \mathbf{S} and the state signal $\hat{\mathbf{x}}(t), t \in [t_0, t_{N-1}]$, are *free optimization parameters*. They are concurrently optimized according to a cost function constructed with the following rationale.

First, the estimated model output $\hat{\mathbf{y}}$ should match the output measurements in training dataset \mathcal{D} . This objective is achieved by introducing a *fitting term* J_y in the cost function which penalizes the mismatch between the model outputs $\hat{\mathbf{y}}(t_k)$ and the sampled measured outputs $\mathbf{y}(t_k)$, $k = 0, 1, \dots, N-1$.

Second, the state signal $\hat{\mathbf{x}}$ should be compatible with the LSS model dynamics (4). This can be achieved through an additional *regularization term* J_x , which penalizes the

distance between $\hat{\mathbf{x}}_I(t)$ and $\hat{\mathbf{x}}(t)$, where $\hat{\mathbf{x}}_I$ is defined as in (5). The regularization term enforces the state $\hat{\mathbf{x}}$ (which is to be optimized) to follow the CT model dynamics (4).

Furthermore, a *mode loss* term $\mathcal{L} : \mathcal{K}^N \rightarrow \mathbb{R}$ (where $\mathcal{K} = \{1, \dots, K\}$) is imposed on the mode sequence \mathbf{S} to take into account the temporal order as well as to incorporate the information of the switching mechanism, for *e.g.*, Markovian switching in jump Markov linear systems etc.

The following minimization problem is thus formulated:

$$\min_{\hat{\mathbf{x}}(\cdot), \mathbf{S}, \Theta_x, \Theta_y} J(\hat{\mathbf{x}}(\cdot), \mathbf{S}, \Theta_x, \Theta_y), \quad (7a)$$

where

$$\begin{aligned} J = & \underbrace{\sum_{k=0}^{N-1} \|\hat{\mathbf{y}}(t_k) - \mathbf{y}(t_k)\|^2}_{J_y} \\ & + \underbrace{\alpha \int_{t_0}^{t_{N-1}} \|\hat{\mathbf{x}}_I(\tau) - \hat{\mathbf{x}}(\tau)\|^2 d\tau}_{J_x} + \beta \mathcal{L}(\mathbf{S}), \end{aligned} \quad (7b)$$

with

$$\hat{\mathbf{y}}(t_k) = \mathcal{M}_y(\hat{\mathbf{x}}(t_k), \mathbf{u}(t_k), \hat{\mathbf{s}}(t_k); \Theta_y(\hat{\mathbf{s}}(t_k))), \quad (7c)$$

$$\hat{\mathbf{x}}_I(t) = \hat{\mathbf{x}}(0) + \int_0^t \mathcal{M}_x(\hat{\mathbf{x}}(\tau), \mathbf{u}(\tau), \hat{\mathbf{s}}(\tau); \Theta_x(\hat{\mathbf{s}}(t_k))) d\tau. \quad (7d)$$

As introduced in (Bemporad et al., 2018), the following mode loss $\mathcal{L} : \mathcal{K}^N \rightarrow \mathbb{R}$ can be considered

$$\begin{aligned} \mathcal{L}(\mathbf{S}) = & \mathcal{L}^{\text{init}}(\hat{\mathbf{s}}(0)) + \sum_{k=1}^{N-1} \mathcal{L}^{\text{mode}}(\hat{\mathbf{s}}(t_k)) \\ & + \sum_{k=1}^{N-1} \mathcal{L}^{\text{trans}}(\hat{\mathbf{s}}(t_k), \hat{\mathbf{s}}(t_{k-1})), \end{aligned} \quad (8)$$

where $\mathcal{K} = \{1, \dots, K\}$, $\mathcal{L}^{\text{init}} : \mathcal{K} \rightarrow \mathbb{R}$ is the initial mode cost, $\mathcal{L}^{\text{mode}} : \mathcal{K} \rightarrow \mathbb{R}$ is the mode cost, and $\mathcal{L}^{\text{trans}} : \mathcal{K}^2 \rightarrow \mathbb{R}$ is the mode transition cost.

The hyper-parameters $\alpha, \beta > 0$ act as a tuning knob balancing the relative importance of the fitting cost J_y , the regularization cost J_x and the *mode loss* $\mathcal{L}(\mathbf{S})$. Additionally, in order to enforce smoothness properties for the estimated state variables, an ℓ_1 regularization term $\|\hat{\mathbf{x}}(t_k) - \hat{\mathbf{x}}(t_{k-1})\|_1$ can be also included in the optimization problem (7a).

3.3 Integral approximation

Note that the continuous-time state signal $\hat{\mathbf{x}}(t) \in \mathbb{R}^{n_x}$, $t \in [t_0, t_{N-1}]$ is one of the problem's decision variables. Indeed, the optimization problem (7) is *infinite-dimensional* and thus computationally intractable. Following the rationale in (Mejari et al., 2022), we employ numerical techniques to approximate (7) into a finite-dimensional problem amenable for a tractable implementation. In particular, the state signal $\hat{\mathbf{x}}(t)$ is approximated using a finite-dimensional parameterization. For simplicity of exposition, we represent the state signal with a *piecewise constant* parameterization, where $\hat{\mathbf{x}}(t)$ is constant during the sampling intervals $[t_{k-1}, t_k]$, $k = 0, 1, \dots, N-1$. In general, more complex parametrizations for $\hat{\mathbf{x}}$ such as piecewise linear

or polynomial could be also used. Moreover, the intervals for the piecewise constant approximation of $\hat{\mathbf{x}}$ may not necessarily correspond to the input/output sampling time Δt or the *dwell time* of the switching signal.

Furthermore, we approximate the integrals in (7b) and (7d) by applying a numerical integration scheme. For simplicity, in this work we apply the classical *rectangular approximation* rule for the numerical integration of (7b) and (7d). Other quadrature rules such as trapezoidal or Gaussian quadrature could be alternatively considered.

Overall, the *piecewise constant* parametrization of the signals $\hat{\mathbf{x}}(t)$, $\mathbf{u}(t)$, $\hat{\mathbf{s}}(t)$ with the *rectangular quadrature* of the integrals leads to the following approximation:

$$\int_{t_0}^{t_{N-1}} \|\hat{\mathbf{x}}_I(\tau) - \hat{\mathbf{x}}(\tau)\|^2 d\tau \approx \sum_{k=1}^{N-1} \|\hat{\mathbf{x}}_I(t_k) - \hat{\mathbf{x}}(t_k)\|^2 \Delta t_k,$$

where $\Delta t_k = t_k - t_{k-1}$, and (7d) can be approximated with the following Riemann sum:

$$\hat{\mathbf{x}}_I(t_k) \approx \hat{\mathbf{x}}(0) + \sum_{j=0}^{k-1} \Delta t_{j+1} \mathcal{M}_x(\hat{\mathbf{x}}(t_j), \mathbf{u}(t_j), \hat{\mathbf{s}}(t_j); \Theta_x(\hat{\mathbf{s}}(t_j))). \quad (9)$$

$$= \hat{\mathbf{x}}(0) + \sum_{j=0}^{k-1} \Delta t_{j+1} \left(\hat{A}_{\hat{\mathbf{s}}(t_j)} \hat{\mathbf{x}}(t_j) + \hat{B}_{\hat{\mathbf{s}}(t_j)} \mathbf{u}(t_j) \right) \quad (10)$$

The sum in the equation above can be also constructed recursively as follows:

$$\hat{\mathbf{x}}_I(t_k+1) = \hat{\mathbf{x}}_I(t_k) + \overbrace{\Delta t_{k+1} \left(\hat{A}_{\hat{\mathbf{s}}(t_k)} \hat{\mathbf{x}}(t_k) + \hat{B}_{\hat{\mathbf{s}}(t_k)} \mathbf{u}(t_k) \right)}^{\Delta \mathbf{x}_k}. \quad (11)$$

3.4 Optimization algorithm

In the following, we present a numerical optimization algorithm in order to minimize the cost function J in (7a) w.r.t. the parameters $\{\hat{\mathbf{x}}, \mathbf{S}, \Theta_x, \Theta_y\}$. To this end, we employ the *coordinate-descent* approach as described in Algorithm 1. With a slight abuse of notation, the optimization variable $\hat{\mathbf{x}}$ in Algorithm 1 denotes the finite-dimensional representation of the state signal $\hat{\mathbf{x}}$, i.e., $\hat{\mathbf{x}} = \{\hat{\mathbf{x}}(t_0), \dots, \hat{\mathbf{x}}(t_{N-1})\}$.

Given an initial guess $\hat{\mathbf{x}}^{(0)}$ of the state and $\mathbf{S}^{(0)}$ of the mode sequence, at each iteration $n \geq 1$, Algorithm 1 alternates between three steps: Step 1.1, Step 1.2 and Step 1.3. In particular, at Step 1.1, model parameters Θ_x, Θ_y are computed by solving (7a) for a *fixed* state $\hat{\mathbf{x}}^{(n-1)}$ and mode sequence $\mathbf{S}^{(n-1)}$ obtained at the iteration $(n-1)$. At Step 1.2, the mode sequence is estimated for *fixed* states $\hat{\mathbf{x}}^{(n-1)}$ and fixed model parameters $\Theta_x^{(n)}$ and $\Theta_y^{(n)}$ obtained from Step 1.1 at the n -th iteration. Subsequently, at Step 1.3, the state sequence $\hat{\mathbf{x}}^{(n)}$ is estimated by minimizing the cost (7a) for *fixed* model parameters $\Theta_x^{(n)}$ and $\Theta_y^{(n)}$ obtained from Step 1.1 and mode sequence $\mathbf{S}^{(n)}$ computed from Step 1.2. The procedure continues until a maximum number of iterations is reached, or a certain convergence criterion is met (Step 2).

Algorithm 1 Block coordinate descent for the estimation of states $\hat{\mathbf{x}}$, mode sequence \mathbf{S} and model parameter matrices Θ_x, Θ_y .

Input: Training dataset $\mathcal{D} = \{\mathbf{u}(t_k), \mathbf{y}(t_k)\}_{k=0}^{N-1}$; initial guess $\hat{\mathbf{x}}^{(0)}, \mathbf{S}^{(0)}$; tuning parameter α, β ; tolerance ϵ , maximum number of iterations n_{\max} .

1. **Iterate for** $n = 1, \dots$
 - 1.1. $\Theta_x^{(n)}, \Theta_y^{(n)} \leftarrow \arg \min_{\Theta_x, \Theta_y} J(\hat{\mathbf{x}}^{(n-1)}, \mathbf{S}^{(n-1)}, \Theta_x, \Theta_y)$
 - 1.2. $\mathbf{S}^{(n)} \leftarrow \operatorname{argmin}_{\mathbf{S}} J(\hat{\mathbf{x}}^{(n-1)}, \mathbf{S}, \Theta_x^{(n)}, \Theta_y^{(n)})$
 - 1.3. $\hat{\mathbf{x}}^{(n)} \leftarrow \operatorname{argmin}_{\hat{\mathbf{x}}} J(\hat{\mathbf{x}}, \mathbf{S}^{(n)}, \Theta_x^{(n)}, \Theta_y^{(n)})$
 2. **Until** $\|J^{(n)} - J^{(n-1)}\| \leq \epsilon$ or $n = n_{\max}$
-

Output: Estimated $\{\hat{\mathbf{x}}(t_k)\}_{k=0}^{N-1}$, \mathbf{S} and Θ_x, Θ_y .

Remark 1. Since the underlying optimization problem is non-convex, convergence of Algorithm 1 to the global optimal is sensitive to the initial guesses for states $\hat{\mathbf{x}}^{(0)}$ and mode sequence $\mathbf{S}^{(0)}$. A possible choice to initialize the state sequence is to first identify a continuous-time LTI state-space model and set $\hat{\mathbf{x}}^{(0)}$ to the states of the LTI model with small additive perturbations, i.e., $\hat{\mathbf{x}}^{(0)} = \hat{\mathbf{x}}_{\text{LTI}} + v_x$ where, $v_x \sim \mathcal{N}(0, \sigma_x^2)$ with variance σ_x^2 chosen by the user. We remark that, in practice, Algorithm 1 can be run multiple times with different initial conditions and then choosing the best model parameters according to a figure of merit.

Remark 2. We stress that in Algorithm 1, Steps 1.1 and 1.3 can be solved *analytically* via ordinary least squares, while Step 1.2 is solved to global optimality via dynamic programming. Thus, each sub-problem to be optimized within an iteration of the block coordinate descent is solved exactly to its unique optimal solution, which can be utilized to prove the convergence guarantees, see (Razaviyayn et al., 2013; Tseng, 2001).

In the following section, we detail each step of the coordinate descent algorithm. Without loss of generality, for brevity, we set $\hat{C}_i = \hat{C}$, $\hat{D}_i = 0$ for all $i = 1, \dots, K$.

Step 1.1: Optimization over model parameters Θ_x, Θ_y
For a fixed mode sequence \mathbf{S} and a fixed state sequence $\hat{\mathbf{x}}$, the cost function $J(\hat{\mathbf{x}}^{(n-1)}, \mathbf{S}^{(n-1)}, \Theta_x, \Theta_y)$ in (7b) can be optimized over the unknown model parameters Θ_x, Θ_y . This leads to a *least-squares* problem described as follows.

Let $\theta_i = \left[\operatorname{vec}(\hat{A}_i)^\top \operatorname{vec}(\hat{B}_i)^\top \right]^\top \in \mathbb{R}^{n_\theta}$, with $n_\theta = n_x(n_x + n_u)$ and let us define the matrix $\Phi(t_j) \in \mathbb{R}^{n_\theta \times n_x}$ as follows

$$\Phi(t_j) = \Delta t \begin{bmatrix} \hat{\mathbf{x}}(t_j) \\ \mathbf{u}(t_j) \end{bmatrix} \otimes I_{n_x} \quad (12)$$

with \otimes denoting the Kronecker product.

The approximated state evolution eq. (9) can be written as,

$$\hat{\mathbf{x}}_I(t_k) \approx \hat{\mathbf{x}}(0) + \sum_{j=0}^{k-1} \Phi^\top(t_j) \theta_{\hat{\mathbf{s}}(t_j)} \quad (13)$$

Let us define the matrix $P \in \mathbb{R}^{(N-1) \times K}$ such that, for each of its row $i = 1, \dots, N-1$, the j -th column is set to 1 if

the active mode at time t_i is $\hat{\mathbf{s}}(t_i) = j$, *i.e.*, the (i, j) -th entry $P_{i,j}$ is defined as

$$P_{i,j} = 1 \text{ if } \hat{\mathbf{s}}(t_i) = j \\ = 0 \text{ otherwise}$$

and let us define $\bar{P} = P \otimes I_{n_\theta} \in \mathbb{R}^{(N-1)n_\theta \times Kn_\theta}$.

With the matrices defined above, the relation (13) can be written in the matrix form as follows:

$$\underbrace{\begin{bmatrix} \hat{\mathbf{x}}_I(t_1) - \hat{\mathbf{x}}(0) \\ \hat{\mathbf{x}}_I(t_2) - \hat{\mathbf{x}}(0) \\ \vdots \\ \hat{\mathbf{x}}_I(t_{N-1}) - \hat{\mathbf{x}}(0) \end{bmatrix}}_{\Delta \hat{\mathbf{x}}} = \underbrace{\begin{bmatrix} \Phi^\top(t_0) & 0 & 0 & \cdots & 0 \\ \Phi^\top(t_0) & \Phi^\top(t_1) & 0 & \cdots & 0 \\ \vdots & \vdots & \vdots & \ddots & \vdots \\ \Phi^\top(t_0) & \Phi^\top(t_1) & \Phi^\top(t_2) & \cdots & \Phi^\top(t_{N-2}) \end{bmatrix}}_{\Psi} \bar{P} \begin{bmatrix} \theta_1 \\ \theta_2 \\ \vdots \\ \theta_K \end{bmatrix} \quad (14)$$

Based on the above definitions, the cost function (7b) can be re-written as

$$J = \underbrace{\|\tilde{C}\hat{\mathbf{x}} - \mathbf{y}\|^2}_{J_y} + \alpha \underbrace{\|\Delta \hat{\mathbf{x}} - \Psi \bar{P} \Theta\|^2}_{J_x} \Delta t \quad (16)$$

where $\tilde{C} = \text{blk}(\hat{C})$ is a block-diagonal matrix, $\hat{\mathbf{x}}$ and \mathbf{y} are the sequences of estimated states and measured outputs respectively. Note that, for a given state estimates $\hat{\mathbf{x}}$ and a given mode sequence \mathbf{S} , the matrices Ψ and \bar{P} can be pre-computed and thus, (16) is a *least-squares* problem in the unknown model parameters $\{\theta_i\}_{i=1}^K, \hat{C}$ (*i.e.*, $\{\hat{A}_i, \hat{B}_i\}_{i=1}^K, \hat{C}$), which can be solved analytically.

Step 1.2: Optimization over mode sequence \mathbf{S} Given the estimates of the model parameters $\{\hat{A}_i, \hat{B}_i\}_{i=1}^K, \hat{C}$ computed at Step 1.1 and given a fixed state sequence $\hat{\mathbf{x}}$, the cost function $J(\hat{\mathbf{x}}^{(n-1)}, \mathbf{S}, \Theta_x^{(n)}, \Theta_y^{(n)})$ in (7b) can be optimized over the unknown mode sequence \mathbf{S} via discrete *Dynamic Programming* (DP) algorithm (Bemporad et al., 2018).

The DP algorithm to estimate the mode sequence \mathbf{S} is summarized as follows. Let $\ell(\hat{\mathbf{x}}(t_k), \mathbf{u}(t_k), \theta_{\hat{\mathbf{s}}(t_k)})$ be the transition cost defined as

$$\ell(\hat{\mathbf{x}}(t_k), \mathbf{u}(t_k), \theta_{\hat{\mathbf{s}}(t_k)}) \\ = \left\| \hat{\mathbf{x}}(t_{k+1}) - \hat{\mathbf{x}}(t_k) - \Delta t \hat{A}_{\hat{\mathbf{s}}(t_k)} \hat{\mathbf{x}}(t_k) - \Delta t \hat{B}_{\hat{\mathbf{s}}(t_k)} \mathbf{u}(t_k) \right\|^2$$

We compute a matrix of cost $V \in \mathbb{R}^{K \times (N+1)}$ and a matrix of indices $U \in \mathbb{R}^{K \times N}$ as follows:

First, the terminal cost $V_{i,N} \in \mathbb{R}$ is computed for all modes $V_{i,N-1} = \mathcal{L}^{\text{mode}}(i) + \ell(\hat{\mathbf{x}}(t_{N-1}), \mathbf{u}(t_{N-1}), \theta_i)$ $i = 1, \dots, K$.

Next, the cost $V_{i,k}$ and indexes $U_{i,k}$ at time t_k are computed with following dynamic programming recursions, backwards in time for $k = N-2, \dots, 1, 0$

$$U(i, k) = \arg \min_{j=1, \dots, K} \{V_{j,k+1} + \mathcal{L}^{\text{trans}}(j, i)\}, \quad i = 1, \dots, K \\ V_{i,k} = \mathcal{L}^{\text{mode}}(i) + \ell(\hat{\mathbf{x}}(t_k), \mathbf{u}(t_k), \theta_i) + V_{U(i,k),k+1} \\ + \mathcal{L}^{\text{trans}}(U(i, k), i), \\ V_{i,0} = \mathcal{L}^{\text{init}}(i) + \min_{j=1, \dots, K} \{V_{j,1} + \mathcal{L}^{\text{trans}}(j, i)\}$$

The minimum cost mode sequence \mathbf{S} is retrieved forward in time by setting

$$\hat{\mathbf{s}}_{t_0} = \arg \min_{j=1, \dots, K} V_{j,0} \\ \hat{\mathbf{s}}_{t_k} = U(\hat{\mathbf{s}}_{t_{k-1}}, k) \quad k = 1, \dots, N-1$$

Step 1.3: Optimization over states $\hat{\mathbf{x}}$ By assuming that the initial conditions $\hat{\mathbf{x}}_I(t_0)$ and $\hat{\mathbf{x}}(t_0)$ are equal, *i.e.*,

$$\hat{\mathbf{x}}_I(t_0) = \hat{\mathbf{x}}(t_0), \quad (17)$$

the relation (11) can be written in the matrix form:

$$\begin{bmatrix} \hat{\mathbf{x}}_I(t_0) \\ \hat{\mathbf{x}}_I(t_1) \\ \hat{\mathbf{x}}_I(t_2) \\ \vdots \\ \hat{\mathbf{x}}_I(t_{N-1}) \end{bmatrix} = \underbrace{\begin{bmatrix} I & 0 & 0 & \cdots & 0 & 0 \\ I + \Delta t \hat{A}_{\hat{\mathbf{s}}(t_0)} & 0 & 0 & \cdots & 0 & 0 \\ I + \Delta t \hat{A}_{\hat{\mathbf{s}}(t_0)} & \Delta t \hat{A}_{\hat{\mathbf{s}}(t_1)} & 0 & \cdots & 0 & 0 \\ \vdots & \vdots & \vdots & \ddots & \vdots & \vdots \\ I + \Delta t \hat{A}_{\hat{\mathbf{s}}(t_0)} & \Delta t \hat{A}_{\hat{\mathbf{s}}(t_1)} & \Delta t \hat{A}_{\hat{\mathbf{s}}(t_2)} & \cdots & \Delta t \hat{A}_{\hat{\mathbf{s}}(t_{N-2})} & 0 \end{bmatrix}}_{\tilde{A}} \begin{bmatrix} \hat{\mathbf{x}}(t_0) \\ \hat{\mathbf{x}}(t_1) \\ \hat{\mathbf{x}}(t_2) \\ \vdots \\ \hat{\mathbf{x}}(t_{N-1}) \end{bmatrix} \\ + \underbrace{\begin{bmatrix} 0 \\ \Delta t \hat{B}_{\hat{\mathbf{s}}(t_0)} \mathbf{u}(t_0) \\ \Delta t \hat{B}_{\hat{\mathbf{s}}(t_0)} \mathbf{u}(t_0) + \Delta t \hat{B}_{\hat{\mathbf{s}}(t_1)} \mathbf{u}(t_1) \\ \vdots \\ \Delta t \hat{B}_{\hat{\mathbf{s}}(t_0)} \mathbf{u}(t_0) + \Delta t \hat{B}_{\hat{\mathbf{s}}(t_1)} \mathbf{u}(t_1) + \dots + \Delta t \hat{B}_{\hat{\mathbf{s}}(t_{N-2})} \mathbf{u}(t_{N-2}) \end{bmatrix}}_{\tilde{B}} \quad (18)$$

Thus, based on the above approximation, the cost function (7b) can be also re-written as

$$J = \underbrace{\|\tilde{C}\hat{\mathbf{x}} - \mathbf{y}\|^2}_{J_y} + \alpha \underbrace{\|(\tilde{A} - I)\hat{\mathbf{x}} + \tilde{B}\|^2}_{J_x} \Delta t + \mathcal{L}(\mathbf{S}), \quad (19)$$

where $\tilde{C} = \text{blk}(C)$, which can be solved for $\hat{\mathbf{x}}$ via ordinary least-squares.

4. SIMULATION EXAMPLE

The performance of the proposed algorithm is assessed via a simulation case study. All computations are carried out on an i7 1.9-GHz Intel core processor with 32 GB of RAM running MATLAB R2019a.

We consider a continuous-time linear switched system governed by (1) having $K = 2$ modes with subsystem matrices given as follows (Goudjil et al., 2020):

$$\left[\begin{array}{c|c} A_1 & B_1 \\ \hline C_1 & D_1 \end{array} \right] = \left[\begin{array}{cc|c} 0 & -120 & 120 \\ 1 & -4 & -12 \\ \hline 0 & 1 & 0 \end{array} \right], \\ \left[\begin{array}{c|c} A_2 & B_2 \\ \hline C_2 & D_2 \end{array} \right] = \left[\begin{array}{cc|c} 0 & -50 & 53 \\ 1 & -1.8 & 25 \\ \hline 0 & 1 & 0 \end{array} \right]$$

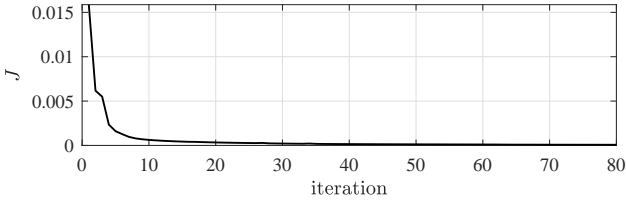


Fig. 2. Training: Cost function *vs* number of iterations.

The system is excited with a zero-mean Gaussian input signal having unit variance, $\mathbf{u}(t) \sim \mathcal{N}(0, 1)$. The dynamics switches between the two subsystems with a Markov switching signal, such that the true mode \mathbf{s}_{t_k} has $\pi = 10\%$ probability of being different from $\mathbf{s}_{t_{k-1}}$, starting from $\mathbf{s}_{t_0} = 1$. The system belongs to a class of switched models termed as continuous-time jump Markov linear systems (Costa et al., 2013). Training dataset of $N = 400$ samples is gathered, sampling the output and input trajectories with a sampling time of $\Delta t = 0.01$ s. The output is corrupted by an additive white Gaussian noise $\mathbf{y}(t_k) = \mathbf{y}^o(t_k) + \eta(t_k)$ where $\eta(t_k) \sim \mathcal{N}(0, \sigma_\eta^2)$ with $\sigma_\eta = 0.025$, which corresponds to signal-to-noise ratio of 30 dB.

For identification, we consider an LSS model structure (4) with state dimension set to the true system dimension $n_x = 2$ and number of modes set to $K = 2$. The model matrices Θ_x , Θ_y , the mode sequence \mathbf{S} and the state sequence $\hat{\mathbf{x}}$ are estimated by running the coordinate descent Algorithm 1 for $n_{\max} = 1000$ iterations. The average computational time for each iteration of the algorithm is 0.1 s, which includes the time to compute the model matrices and states via ordinary least-squares and estimation of mode sequence via dynamic programming recursions. In total, the entire identification problem is completed in about 500 s, with 5 different initial guesses.

To assess the convergence properties, cost J is plotted in Fig. 2 against the iterations of the coordinate descent algorithm.

As mentioned in Remark 1, the initial guess $\hat{\mathbf{x}}^{(0)}$ for the state sequence is set to the states of an identified CT LTI state-space model¹ with small additive perturbations, *i.e.*, $\hat{\mathbf{x}}^{(0)} = \hat{\mathbf{x}}_{\text{LTI}} + v_x$ where, $v_x \sim \mathcal{N}(0, \sigma_x^2 I)$ with $\sigma_x = 0.01$. The initial guess for the mode sequence $\mathbf{S}^{(0)}$ is chosen randomly.

For the mode loss $\mathcal{L}(\mathbf{S})$ (see eq. (8)), we set initial mode cost $\mathcal{L}^{\text{init}}(\mathbf{s}_{t_0}) = 0$, mode cost $\mathcal{L}^{\text{mode}}(\mathbf{s}_{t_k}) = 0$. The transition mode cost $\mathcal{L}^{\text{trans}}$ is chosen as follows:

$$\mathcal{L}^{\text{trans}}(\mathbf{s}_{t_k}, \mathbf{s}_{t_{k-1}}) = \begin{cases} -\tau \log(1 - \pi) & \text{if } \mathbf{s}_{t_k} = \mathbf{s}_{t_{k-1}} \\ \tau \log(\pi) & \text{if } \mathbf{s}_{t_k} \neq \mathbf{s}_{t_{k-1}} \end{cases} \quad (20)$$

with $\pi = 0.1$ and $\tau = 10^{-6}$. The regularization hyper-parameter α is set to 0.01. The hyper-parameters τ and α are chosen via a grid search.

The true and estimated transfer functions $G(s)$ of the two linear subsystems are reported in Table 1. The corresponding Bode plots of the subsystems are depicted in Fig. 3. The obtained results show that the model parameters of

¹ The CT LTI model is identified using MATLAB's system identification toolbox with command `sstest` which employs N4SID subspace algorithm.

Table 1. True *vs* estimated transfer functions for mode 1 and mode 2.

Mode	True	Estimated
$G_1(s)$	$\frac{-12s+120}{s^2+4s+120}$	$\frac{-12.01s+122.3}{s^2+3.98s+119}$
$G_2(s)$	$\frac{25s+53}{s^2+1.8s+50}$	$\frac{24.97s+52.9}{s^2+1.89s+49.3}$

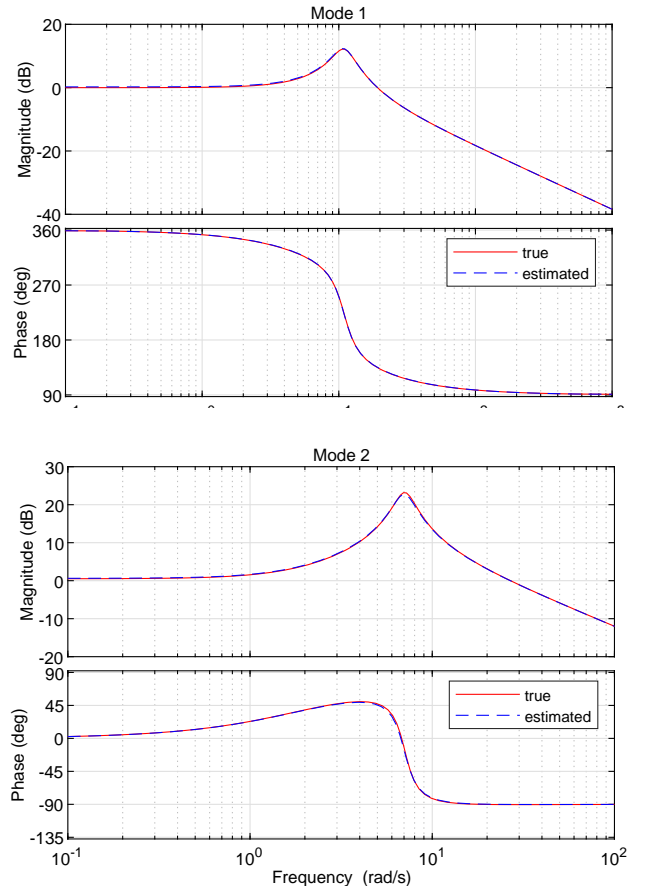


Fig. 3. Bode plot: true (red) *vs* estimated (dashed blue) model for mode 1 (top panel) and mode 2 (bottom panel).

each subsystem have been identified with high accuracy and input-output behavior of the estimated linear subsystems matches closely to that of the true subsystems.

The performance of the proposed identification algorithm is further assessed in terms of mode sequence estimation, quantified via a *mode fit* (MF) index $\frac{100}{N} \sum_{k=0}^{N-1} \delta(\hat{\mathbf{s}}_{t_k}, \mathbf{s}_{t_k})$ where $\delta(i, j)$ is the Kronecker delta function. Fig. 4 shows the true *vs* the estimated mode sequence. Only 7 out of 400 modes have been incorrectly classified which leads to a mode fit of 98.25%. It is clear from Fig. 4 that, starting from a random initial mode sequence, the proposed algorithm is able to reconstruct the true mode sequence accurately.

Furthermore, we assess the effect of varying noise levels σ_η as well as regularization hyper-parameters τ on the performance of the proposed algorithm quantified via mode-fit index. The results are summarized in Fig. 5, which shows the percentage of correctly classified modes against the

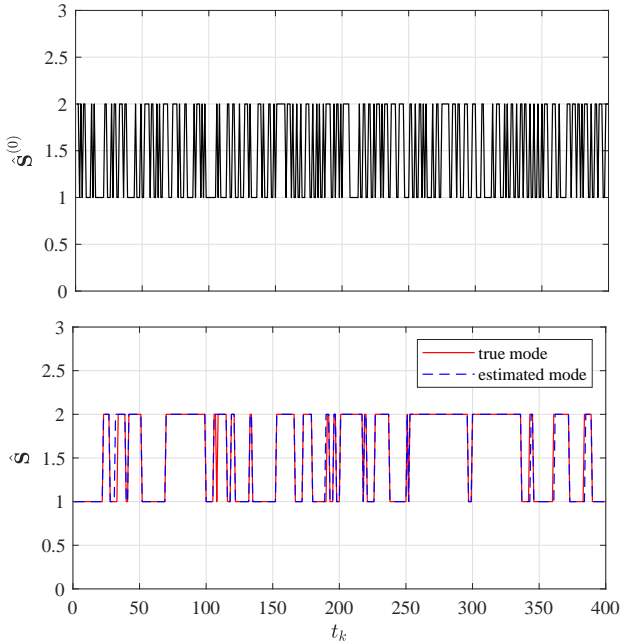


Fig. 4. Estimation of mode sequence: Top panel: Random initial guess $\hat{\mathbf{S}}^{(0)}$, Bottom panel: True (red) *vs* estimated (blue) mode sequence with mode fit percent = 98.25%.

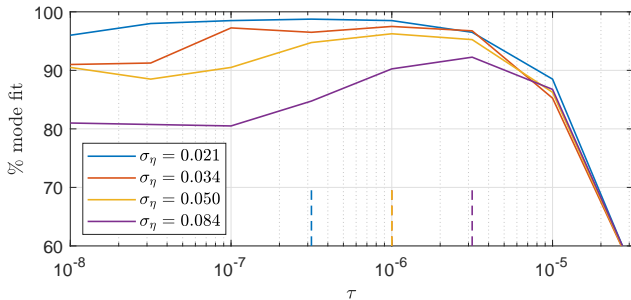


Fig. 5. Mode fit percent *vs* τ for different noise levels. Optimal value of τ shown with dashed lines.

values of τ for different noise standard deviations $\sigma_\eta = \{0.02, 0.03, 0.05, 0.08\}$ corresponding to signal-to-noise ratios $\{32, 28, 24, 20\}$ dB, respectively. From the choice of the mode transition loss $\mathcal{L}^{\text{trans}}$ in (20), higher values of τ implies more penalty on the change of mode. In other words, for large values of τ , mode change is discouraged and only single mode is recognized (typically, the value of the initial mode $\hat{\mathbf{s}}_{t_0}$ is retained), leading to a lower mode fit percent as seen in Fig. 5. The hyperparameter τ and the choice of $\mathcal{L}^{\text{trans}}$ thus act as a tuning knob, which can be chosen via cross-validation, depending upon either fast or slow switching dynamics.

Finally, in order to analyze the statistical properties and robustness of the proposed algorithm, we perform a Monte-Carlo (MC) analyses with 50 MC runs. At each MC run, data is gathered by exciting the system with a new realization of the input, switching signal and noise. The variance of the noise distribution is set such that the average SNR for each run is 30 dB. Algorithm 1 is run for 5 different initial guesses for the states $\hat{\mathbf{x}}^{(0)}$ and mode sequence $\hat{\mathbf{S}}^{(0)}$, with $n_{\text{max}} = 1000$ iterations setting $(\alpha, \tau) = (0.01, 3 \cdot 10^{-7})$. Among 5 different initializations,

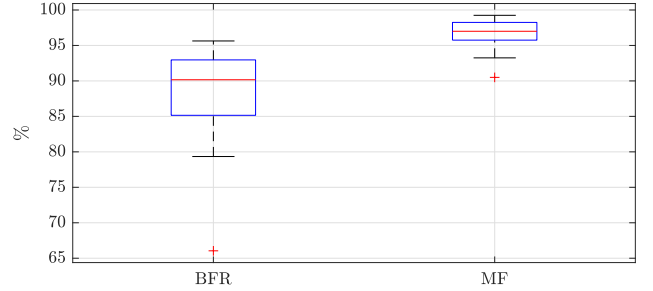


Fig. 6. Monte-Carlo analysis: Best fit rate and mode fit percentage over 50 MC runs.

model parameters obtained from the run having maximum *best fit rate*: $\text{BFR} = 100 \left(1 - \sqrt{\frac{\sum_{k=0}^{N-1} (\hat{\mathbf{y}}(t_k) - \mathbf{y}(t_k))^2}{\sum_{k=0}^{N-1} (\mathbf{y}(t_k) - \bar{\mathbf{y}})^2}} \right) \%$ are chosen.

The box-plots of the mode fit (MF) and BFR indexes over 50 Monte-Carlo runs are shown in Fig. 6. We observe that satisfactory performance is obtained in terms of reconstruction of the output as well as the mode sequence. We remark that, although convergence is not guaranteed for every run of the algorithm, in practice, running the algorithm with 5 different initializations was sufficient to achieve accurate model parameter estimates.

5. CONCLUSIONS

In this work, we have presented an integral architecture for continuous-time identification of switched state-space models. The proposed approach can be seen as the first step towards developing a generic framework for direct identification of continuous-time state-space hybrid dynamical systems. The presented analysis has shown that satisfactory results have been achieved for identifying a Markov jump linear system, in terms of reconstruction of the mode sequence as well as capturing the input-output behaviours of the linear submodels. Future works will focus on developing refinement strategies in order to improve the estimation of mode sequence and robustness w.r.t. to initial conditions.

REFERENCES

- Abdollahi, F. and Khorasani, K. (2011). A decentralized markovian jump \mathcal{H}_∞ control routing strategy for mobile multi-agent networked systems. *IEEE Transactions on Control Systems Technology*, 19(2), 269–283.
- Bako, L. (2011). Identification of switched linear systems via sparse optimization. *Automatica*, 47(4), 668 – 677.
- Bako, L., Mercère, G., Vidal, R., and Lecoeuche, S. (2009). Identification of switched linear state space models without minimum dwell time. In *Proc. 15th IFAC Symposium on System Identification*, 569–574. Saint-Malo, France.
- Bemporad, A., Breschi, V., Piga, D., and Boyd, S. (2018). Fitting jump models. *Automatica*, 96, 11–21.
- Breschi, V., Piga, D., and Bemporad, A. (2016). Piecewise affine regression via recursive multiple least squares and multicategory discrimination. *Automatica*, 73, 155–162.
- Costa, O.L.V., Fragoso, M.D., and Todorov, M.G. (2013). *Continuous-Time Markov Jump Linear Systems*. Springer.

- Doucet, A., Gordon, N., and Krishnamurthy, V. (2001). Particle filters for state estimation of jump markov linear systems. *IEEE Transactions on Signal Processing*, 49(3), 613–624.
- Du, Y., Liu, F., Qiu, J., and Buss, M. (2021). Online identification of piecewise affine systems using integral concurrent learning. *IEEE Transactions on Circuits and Systems I: Regular Papers*, 68(10), 4324–4336.
- Garnier, H. (2015). Direct continuous-time approaches to system identification. overview and benefits for practical applications. *European Journal of control*, 24, 50–62.
- Garnier, H. and Wang, L. (2008). *Identification of Continuous-time Models from Sampled Data*. Springer Publishing Company.
- Goudjil, A., Pouliquen, M., Pigeon, E., Gehan, O., and Bonargent, T. (2020). Continuous-time identification for a class of switched linear systems. In *Proc. 2020 European Control Conference (ECC)*, 521–526. Saint Petersburg, Russia.
- Kersting, S. and Buss, M. (2019). Recursive estimation in piecewise affine systems using parameter identifiers and concurrent learning. *International Journal of Control*, 92(6), 1264–1281.
- Mavkov, B., Forgiione, M., and Piga, D. (2020). Integrated neural networks for nonlinear continuous-time system identification. *IEEE Control Systems Letters*, 4(4), 851–856.
- Mejari, M., Breschi, V., and Piga, D. (2020a). Recursive bias-correction method for identification of piecewise affine output-error models. *IEEE Control Systems Letters*, 4(4), 970–975.
- Mejari, M., Mavkov, B., Forgiione, M., and Piga, D. (2022). Direct identification of continuous-time LPV state-space models via an integral architecture. *Automatica*, 142, 110407.
- Mejari, M., Naik, V.V., Piga, D., and Bemporad, A. (2018). Energy disaggregation using piecewise affine regression and binary quadratic programming. In *Proc. 57th IEEE Conference on Decision and Control (CDC)*, 3116–3121. Miami Beach, FL, USA.
- Mejari, M., Naik, V.V., Piga, D., and Bemporad, A. (2020b). Identification of hybrid and linear parameter-varying models via piecewise affine regression using mixed integer programming. *International Journal of Robust and Nonlinear Control*, 30(15), 5802–5819.
- Oh, S.M., Rehg, J.M., Balch, T., and Dellaert, F. (2008). Learning and inferring motion patterns using parametric segmental switching linear dynamic systems. *International Journal of Computer Vision*, 77, 103–124.
- Ohlsson, H. and Ljung, L. (2013). Identification of switched linear regression models using sum-of-norms regularization. *Automatica*, 49(4), 1045–1050.
- Pavlovic, V., Rehg, J.M., and MacCormick, J. (2000). Learning switching linear models of human motion. In *Proc. of the 13th International Conference on Neural Information Processing Systems*, 942–948. Denver CO, United States.
- Petreczky, M., Bako, L., and van Schuppen, J.H. (2013). Realization theory of discrete-time linear switched systems. *Automatica*, 49(11), 3337–3344.
- Piga, D. (2018). Finite-horizon integration for continuous-time identification: bias analysis and application to variable stiffness actuators. *International Journal of Control*, 93.
- Piga, D., Bemporad, A., and Benavoli, A. (2020). Rao-Blackwellized sampling for batch and recursive Bayesian inference of Piecewise Affine models. *Automatica*, 117, 109002.
- Razaviyayn, M., Hong, M., and Luo, Z. (2013). A unified convergence analysis of block successive minimization methods for nonsmooth optimization. *SIAM Journal on Optimization*, 23(2), 1126–1153.
- Tseng, P. (2001). Convergence of a block coordinate descent method for nondifferentiable minimization. *Journal of Optimization Theory and Applications*, 109, 475–494.
- Verdult, V. and Verhaegen, M. (2004). Subspace identification of piecewise linear systems. In *Proc. 43rd IEEE Conference on Decision and Control (CDC)*, volume 4, 3838–3843. Atlantis, Bahamas.
- Vidal, R. (2008). Recursive identification of switched ARX systems. *Automatica*, 44(9), 2274–2287.